# Dual-channel Internet-driven controller for a coherent Doppler wind lidar

**A.P. Rostov**

*Institute of Atmospheric Optics,*
*Siberian Branch of the Russian Academy of Sciences, Tomsk*

Received January 25, 2005

A dual-channel controller developed for a Doppler wind lidar and system software for its control via Internet is described.

## Introduction

Since 1970, Doppler lidars have found wide application to atmospheric research and, in particular, to studies of the planetary boundary layer (Refs. 1–7). In recent years, much efforts have been applied to the study of representativeness of wind speed measurements performed with coherent Doppler lidars and to development of the techniques to measure parameters of the atmospheric turbulence from the estimates of wind speed with coherent lidars using cw and pulsed laser radiation. Detailed theoretical and experimental research of the efficiency of coherent wind lidars in application to atmospheric studies have been reported in Refs. 8 to 25. Some results in this field have also been obtained under the project for a cooperative research work between the Institute of Atmospheric Optics SB RAS and the Institute of Atmospheric Physics of the German Aerospace Center (Deutsches Fernerkundungsdatenzentrum, Oberpfaffenhofen, Germany) (Refs. 26–37). For further cooperation, the idea was accepted of developing a coherent Doppler wind lidar at IAO based on the optical elements of an ADOLAR lidar (Ref. 38) developed at the German Institute of Atmospheric Physics in late eighties.

By the end of year 2002, optical elements of the ADOLAR prototype with a cw laser produced by Ferranti Co. were delivered to IAO, where the instrument was equipped with the necessary optics and a receiving-transmitting telescope developed at the IAO. The lidar prototype is shown in Fig. 1.

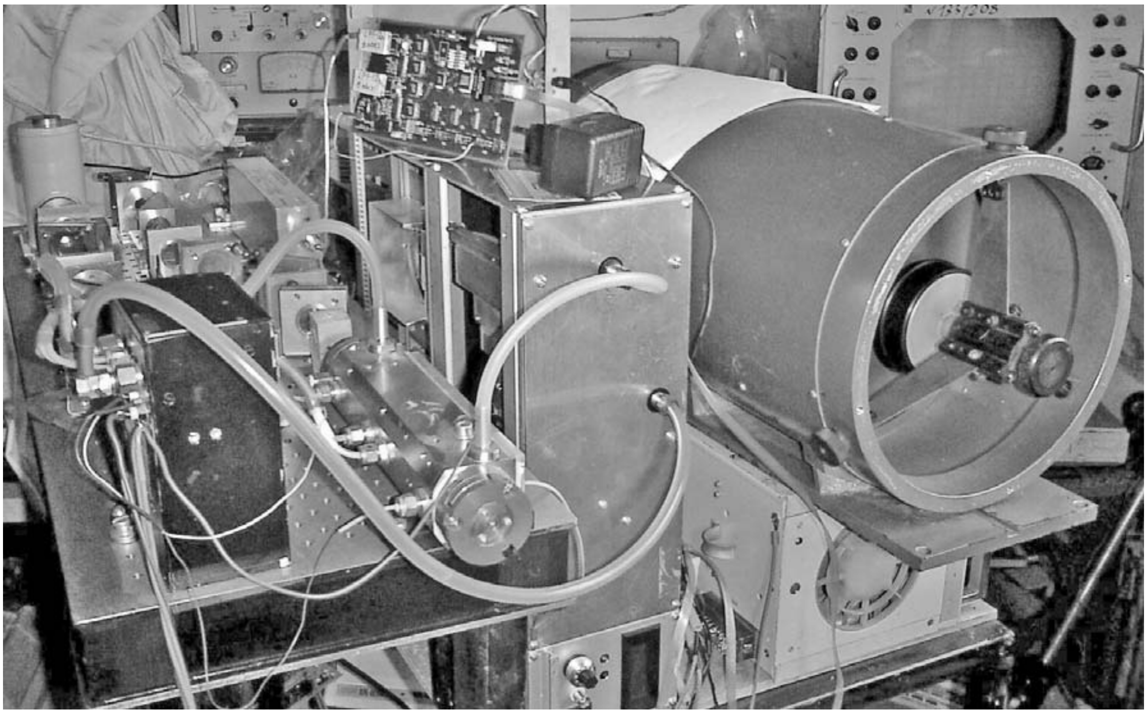

**Fig. 1.** Doppler wind lidar.

0235-6880/06/01 69-07 $02.00 

In addition, it was necessary to develop a controller for data acquisition and recording and for control of the mechano-optical system of the lidar.

During the past twenty years we have developed more than ten controllers for different-purpose lidars. So, the idea of developing similar device for a Doppler lidar making it controllable from any point worldwide seemed quite attractive. In this article, we describe such a device, which was developed with a new control interface and modern electronic components compared to that used in our previous developments.

## Description of the structure scheme

Normally, the structure of aerosol lidar controllers involves an ADC (analog-to-digital converter), a RAM (random access memory), control and synchronization logic circuitries, a crystal oscillator (clock generator), and a controller of an interface for data transmission to a PC. Some models also have controllers of lidar servomechanisms and of laser parameters (Ref. 39).

Having made this traditional controller structure basic, we decided to upgrade it with an interface, which would allow us to remotely control lidar operation. The Ethernet interface was most suitable for this purpose.

It has a galvanic isolation up to 2 kV, which is essential for operation under tough conditions of electromagnetic interference fields. The length of a segment can reach 150 m if a reasonably priced twisted pair category 3 cable is used. This distance is long enough. For example, a lidar equipped with such a controller can be mounted on a high unattended tower.

Dynamic range of the return signal of Doppler lidars does not exceed 70 dB. Therefore, a 12-bit ADC will suffice to digitize the lidar return.

As known, the Doppler frequency shift of radiation reflected from an object depends on the speed of this object:

$$f_d = 2V/\lambda,$$

where $V$ is the object speed; $\lambda$ is the laser radiation wavelength.

From simple calculations, we can find that the frequency range of the signal recorded with a Doppler cw $CO_2$-laser lidar at 10.6 μm wavelength and at a wind speed from 0 to 80 m/s is within the range from 0 to 15 MHz. Taking into account that in calculating wind speed from Doppler lidar returns we shall use the frequency analysis, we need at least to double the discretization frequency. Hence, for our controller it will be quite enough to provide a 12-bit ADC with a conversion frequency higher than 30 MHz.

The designed controller can also be applied to other aerosol lidars. Having this in mind, we have assumed in the controller structure the possibility of replacing the ADC for a faster and precise one. For this purpose, instead of a simple crystal oscillator we used an integral digital frequency multiplier with a built-in crystal oscillator. This allowed us to vary the ADC clock frequency from 4 to 80 MHz.

We have also applied a quick, up to 10 ns, FIFO (First Input First Output) memory with a 16-bit input-output (Ref. 40). The total memory capacity can be up to 32 Kbite per channel and depends only on the FIFO memory chip of this type.

To arrange functioning of the controller components, we needed a fast processor, which would provide transferring data from the FIFO memory to the Ethernet interface controller at the highest possible rate, as well as operative control of the lidar servomechanisms and components, such as laser and its cooling system.

In our earlier developments we have successfully applied modern RISC microcontrollers (Reduced Instruction Set Computer) produced by ATMEL (Ref. 41). These are reliable and fast processors. The most suitable and reasonably priced solution was an ATmega-16 microcontroller released in 2003. These microcontrollers are 8-bit and have a 16 Kbyte Flash-memory. The AVR-kernel of this microcontroller is based on the improved RISC-architecture with a rapid-access register file containing 32 general-purpose registers directly connected to the arithmetic and logic unit (ALU), and an advanced machine-instruction code. It allows two operands to be found in and retrieved from a register file an instruction executed, and the result saved in an appropriate register during single clock cycle. This highly efficient architecture possesses a tenfold higher productivity than the standard CISC microcontrollers.

It has a set of 131 instructions, most of which are executed within one clock cycle. The capacity of the internal programmable Flash-memory is 16 Kbytes, the number of write/erase cycles is 1000. There is also a SPI-interface for internal programming in it. The capacity of the built-in EEPROM is 512 bytes, 100000 write/erase cycles. There is also built-in RAM of 1 Kbyte capacity, with 32 8-bit general-purpose registers, a set of peripheral control registers, 32 programmable I/O lines, serial programmable UART and SPI interfaces. Supply voltage ranges from 2.7 to 6.0 V, and clock rate ranges from 0 to 16 MHz. The efficiency reaches 16 MIPS at a frequency of 16 MHz. To obtain time intervals and organize the analog output, there are two 8-bit timers with a separate pre-divider and an 8-, 9-, or 10-bit pulse-width modulator. Program reliability is attained with a programmable watchdog timer with a built-in generator. To acquire analog signals, there is an analog comparator and an 8-channel 10-bit ADC.

Then, we needed to choose an Ethernet controller for our device. The assortment of Ethernet controllers is not rich. Most of them are designed to run in PC ISA-16 and with PCI buses. Recently, there have appeared 10/100 Mbit/s chips with the Media Independent Interface, but their maintenance requires much faster processors, which would considerably enhance costs. Five years ago, the CRYSTALL company has released an interesting Ethernet controller CS8900A (Ref. 42). Small chip dimensions and built-in filtration circuitries allow one to save space on the card of target device. These chip properties allow us to develop a competitive technical solution in the high-performance Ethernet communication. It operates with an 8-bit bus, which is very convenient for mobile microprocessor systems.

The CS8900A chip in an 8-bit operation mode is controlled via its eight 16-bit ports.

| Shift | Type | Name |
|---|---|---|
| 0000h | Read/Write | Receive/Transmit Data (Port0) |
| 0002h | Read /Write | Receive/Transmit Data (Port1) |
| 0004h | Write | TxCMD (Transmit Command) |
| 0006h | Write | TxLength (Transmit Length) |
| 0008h | Read only | Interrupt Status Queue |
| 000Ah | Read/Write | PacketPage Pointer |
| 000Ch | Read/Write | PacketPage Data (Port 0) |
| 000Eh | Read/Write | PacketPage Data (Port 1) |

In the systems that do not use ISA bus, these addresses normally go to the system's data memory domain. To be taken into account is that the program driver must be able to read or write both data bytes/addresses when it accesses any 16-bit CS8900A register.

Taking into account previously mentioned, we have developed a structure diagram of the controller shown in Fig. 2.

Port B of the controller is used as a bi-directional 8-bit bus. Lower order east bits of the port A (PA0-PA3) shift between the read/write modes and handle the Ethernet interrupt controller. Four lower order bits of port B operate as a unidirectional address bus, and higher order bits control the FIFO memory read mode.

A requirement in digitizing noisy analog signals is application of low pass filters (LPF) at ADC input (Ref. 43). Since we deal with high enough frequencies, application of active filters is impossible due to their slow response. For a Doppler lidar, whose ADC clock rate is 32 MHz, we have developed and manufactured a passive sixth-order LPF with a cutoff frequency of 15 MHz.

The controller operation is maintained via in-system software. The latter has three main modules. The first one runs exchange of information with the controller via the Internet and supports three protocols essential for operation in this network, namely, Address Resolution Protocol (ARP), Internet Control Message Protocol (ICMP), and User Datagram Protocol (UDP) (Ref. 44). This module also configures Ethernet chip at the switch-on point.

An Internet address or, in other words, a Medium Access Control (MAC) address, and an IP address are assigned to the controller while programming an internal ROM of the microcontroller.

A MAC address is a unique number, 48 bits in length, assigned to the network device by the producer. An IP-address is a 4-bit address of a device in a concrete Internet segment.

To accelerate processing of the interrupts of CS8900A Ethernet controller, its query goes directly to the third input of the port A of the microcontroller, and not to the interrupts receiving input. This gives us an approx. 374 ns time advantage in processing an interrupt in each query.

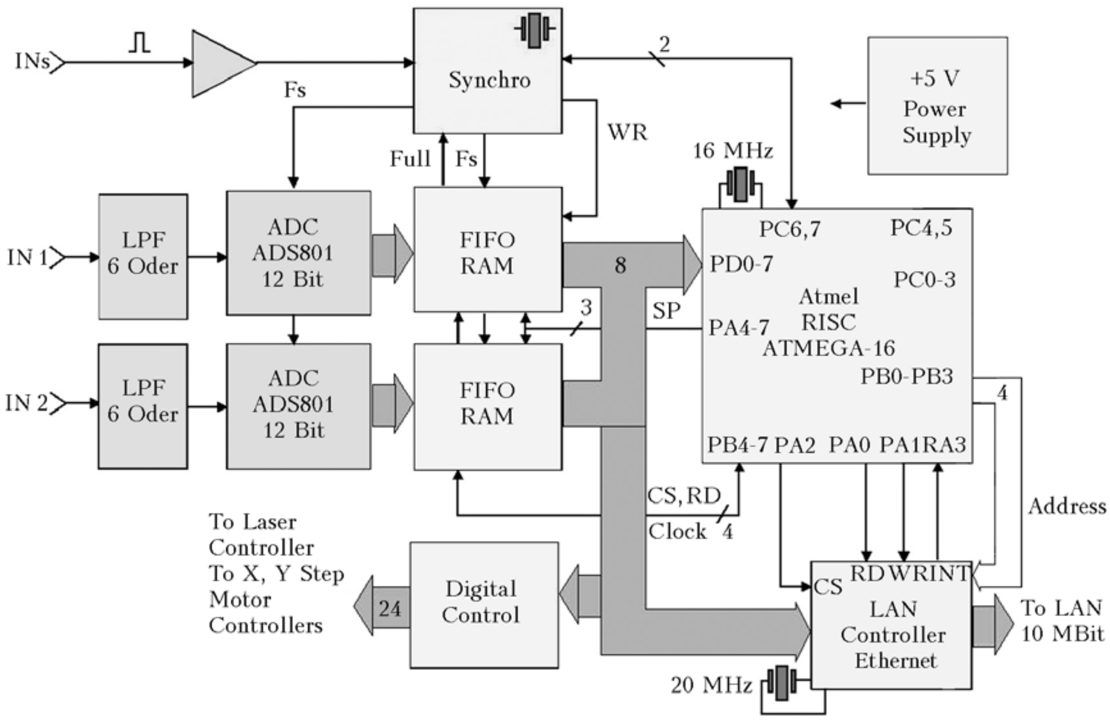


**Fig. 2**. Controller structure scheme.

In addition, we totally control this query, which is very important in maintaining a real time operation of the whole device.

The second program unit is designed to control digitizing of the incoming return signals and to transfer the received data array from the FIFO memory to the output buffer.

The third unit is a dialog with the user. The controller supports 13 working and 3 red-tape instructions. The list and content of the instructions are given in the Table.

These are basic instructions. Controller ROM capacity allows us to increase their number to that required for a specific lidar.

| Instruction number | Instruction | Instruction Hex-code | Comments |
|---|---|---|---|
| 1 | Enable synchronous ADC start | 0x0D | Enables activation of digitizing of signals from two channels by an external pulse. |
| 2 | Disable synchronous ADC start | 0x0E | Disables activation of digitizing |
| 3 | Establish IP connection (handshaking) | 0x55 | The controller remembers the user computer IP and MAC addresses |
| 4 | Output the FIFO-1 content to a user | 0x10 | The controller arranges a multipackage transfer of data from the FIFO-1 memory data array to a user via Internet under the UDP protocol |
| 5 | Output the FIFO-2 content to a user | 0x11 | The controller arranges a multipackage transfer of data from the FIFO-2 memory data array to a user via Internet under the UDP protocol |
| 6 | Set the FIFO memory address counter to "zero" | 0xB | The controller zeros the internal address counter of both units of the FIFO memory |
| 7 | Output the current 128-word (256-byte) data block from FIFO-1 to the user | 0x0C | The controller arranges reading of one current block of the FIFO-1 memory and its transmission to the user via Internet |
| 8 | Output the current 128-word (256-byte) data block from FIFO-2 to the user | 0x0A | The controller arranges reading of one current block of the FIFO-2 memory and its Internet transmission to the user |
| 9 | Read the byte from the microcontroller address space | 0x01 + 2 bytes of the address | Reads the byte from the specified address and transmits it to the user via Internet |
| 10 | Write the byte to the microcontroller address space | 0x02 + 2 bytes of the address + 1 data byte | Writes the byte to the instruction-specified address. Operates via Internet |
| 11 | Read current data buffer | 0x24 | Reads and transmits the data buffer under the UDP protocol to the user via Internet |
| 12 | Set the azimuth drive to the initial position | 0x13 | Sends step pulses and voltage of controller-directed azimuth stepper motor until the rotation stop sensor responds |
| 13 | Set the elevation angle drive to the initial position | 0x14 | Sends step pulses and voltage of controller-directed location angle stepper motor until the rotation stop sensor responds |
| 14 | Set drive to a specified position | 0x15 | Sends certain number of pulses and a corresponding level of a signal to controllers of the elevation and azimuth angle drives |
| 15 | Start scan mirror action | 0x16 | Enables start of the motor rotating the scan mirror of the lidar optical channel |
| 16 | Stop scan mirror action | 0x17 | Stops the motor rotating the scan mirror of the lidar optical channel |

## Controller structure

Taking into account that the controller involves high-frequency devices (up to 80 MHz), we have developed a four-layer printed circuit card (PCC) to reduce electromagnetic interference of the digital controller part in its analog part. The inner conducting layers of the PCC are made solid and simultaneously serve a power bus. Controller tests have proved that this construction works well. Bypass capacitors were uniformly distributed over the whole area of the PCC, which also lowered the emission level of controller power buses. Finally, we have had a compact device of $220 \times 100 \times 30$ mm$^3$ size.

## Controller tests

The controller was tested for accuracy, stability, and reliability of its operation. Its climate sensitivity was tested as well. Sinusoidal voltage of 500 kHz frequency was applied to the controller inputs from a G4-146 generator. The voltage amplitude was chosen to activate the entire ADC bit range. The data obtained are shown in Fig. 3. There are no visible signal distortions.

To determine the level of distortions more accurately, we performed a spectral analysis using a Fast Fourier Transform method. The result is shown in Fig. 4, wherefrom one can see that the level of harmonics does not exceed 70 dB.

To check the level of the controller noise a low-amplitude sinusoidal voltage was applied to its input. The digitized waveform of the input signal is shown in Fig. 5. From this figure one can see that the controller noise does not exceed the level of a lower order bit of the ADC.

In summer of 2004, the controller was installed in the Doppler lidar, with which we conducted several measurements of the wind speed. Controller performance was stable. A fragment of the signal at the Doppler frequency is shown in Fig. 6.

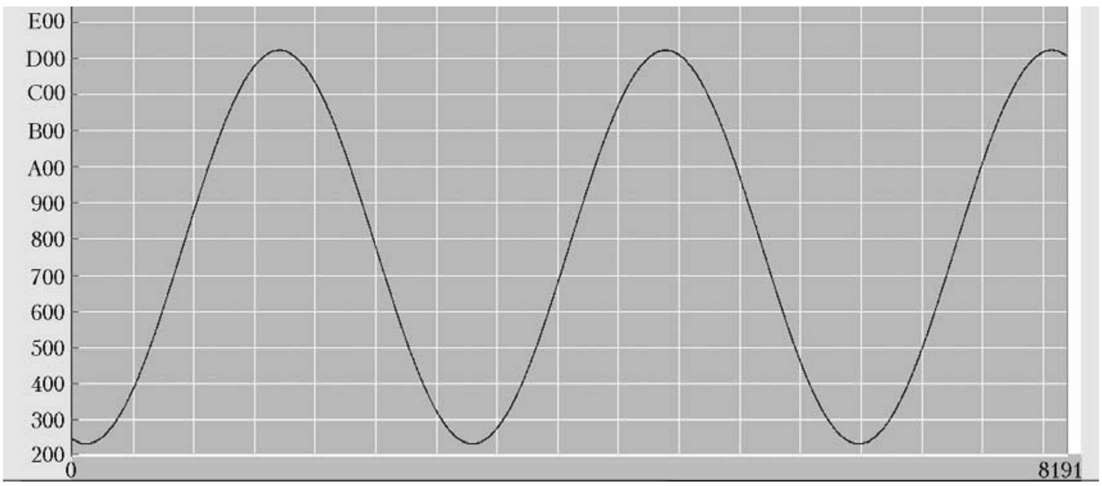


**Fig. 3.** The result of digitizing a large amplitude sinusoidal voltage.

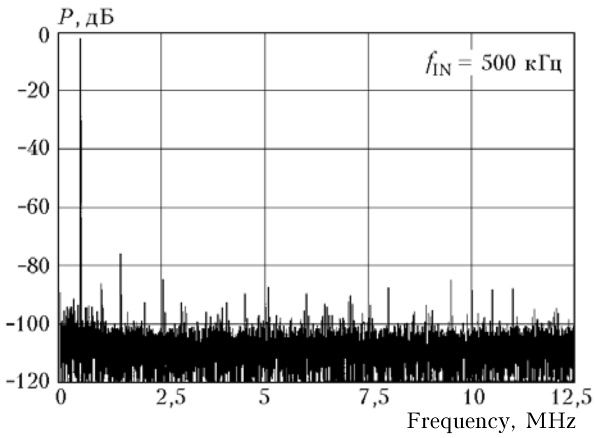


**Fig. 4.** Spectral distribution of the digitizing signal of controller of a large amplitude 500 kHz sinusoidal signal.


**Fig. 5.** The result of digitizing a small amplitude sinusoidal voltage.

Figure 7 shows the power spectrum of this signal. Having done some calculations, which consisted in smoothing the spectrum and finding its maximum, we obtained a time series for the wind component along the optical path at the point the laser beam was focused ($L_f$ = 100 m), shown Fig. 8.

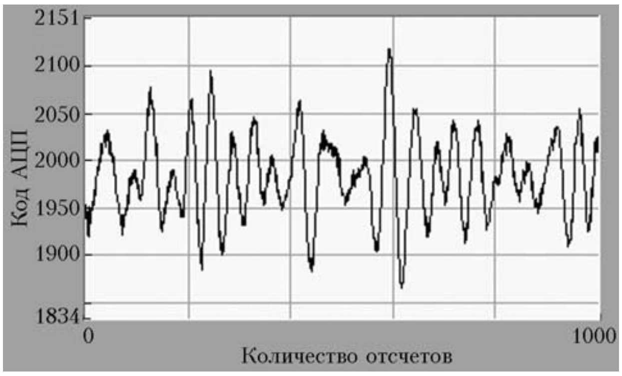


**Fig. 6.** Return signal at the Doppler frequency of a 10.6 μm $CO_2$-laser.

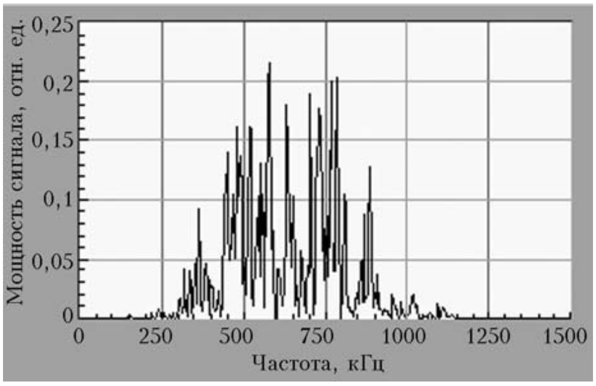


**Fig. 7.** Power spectrum of the return signal at the Doppler frequency of 10.6 μm $CO_2$-laser at the wind speed of 3 m/s.

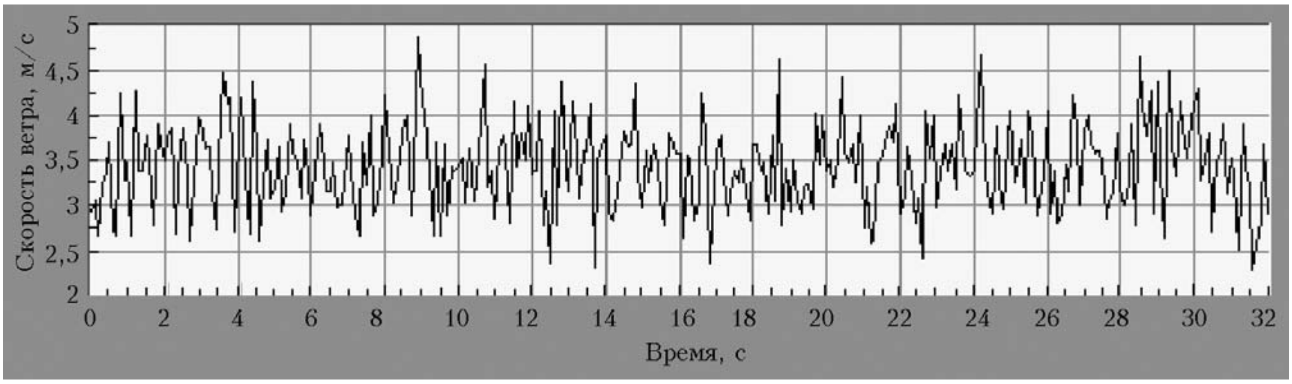


**Fig. 8.** Time series for wind speed calculated from data obtained with a Doppler lidar.

## Summary

The controller we have developed has all the properties and functions needed for operation as a part of a coherent Doppler lidar or any other aerosol lidar. Its first approbation demonstrated a safe control through Ethernet interface via local network as well as via Internet.

### Acknowledgments

The work has been accomplished under financial support of the Russian Foundation for Basic Research (Project No. 03-05-64194).

### References

1. S.W. Henderson, P.J.M. Suni, C.P. Hale, S.M. Hannon, J.R. Magee, D.L. Bruns, and E.H. Yuen, IEEE Trans. Geosci. and Remote Sens. **31**, 4–15 (1993).
2. S.F. Clifford, J.C. Kaimal, R.J. Lataitis, and R.G. Strauch, Proc. IEEE **82**, 313–355 (1994).
3. M.R. Huffaker and R.M. Hardesty, Proc. IEEE **84**, 181–204 (1996).
4. J.M. Vaughan, O. Steinvall, C. Werner, and P.H. Flamant, Proc. IEEE **84**, 205–226 (1996).
5. J.M. Wilczak, E.E. Gossard, W.D. Neff, and W.L. Eberhard, Boundary-Layer Meteorol. **78**, 321–349 (1996).
6. Ch. Werner, P.H. Flamant, O. Reitebuch, F. Kopp, J. Streicher, S. Rahm, E. Nagel, M. Klier, H. Herrmann, C. Loth, P. Delville, Ph. Drobinski, B. Romand, Ch. Boitel, D. Oh, M. Lopez, M. Meissonnier, D. Bruneau, and A. Dabas, Opt. Eng. **40**, 115–125 (2001).
7. O. Reitebuch, Ch. Werner, I. Leike, P. Delville, P. Flamant, A. Cress, and D. Engelbart, J. Atmos. Ocean. Technol. **18**, 1331–1344 (2001).
8. R. Frehlich, S. Hannon, and S. Henderson, Appl. Opt. **36**, 3491–3499 (1997).
9. R. Frehlich, S. Hannon, and S. Henderson, Boundary-Layer Meteorol. **86**, 233–256 (1998).
10. Ph. Drobinski, A. Dabas, and P.H. Flamant, J. Appl. Meteorol. **39**, 2434–2451 (2000).
11. Ph. Drobinski et al., in: *Reviewed and Revised Papers Presented at the Twenty-First International Laser Radar Conference (ILRC21)*, L.R. Bissonnette, G. Roy, and G. Vallee, eds., Quebec, Canada, 8–12 July 2002, pp. 853–856.
12. O. Reitebuch, H. Volkert, Ch. Werner, A. Dabas, P. Delville, Ph. Drobinski, P.H. Flamant, and E. Richard, Quart. J. Roy. Meteorol. Soc. **129**, 715–728 (2003).
13. F. Davies, G.G. Collier, G.N. Pearson, and K.E. Bozier, J. Atmos. Ocean. Technol. **21**, 753–761 (2004).
14. R.G. Frehlich and M.J. Kavaya, Appl. Opt. **30**, No. 36, 5325–5352 (1991).
15. R.G. Frehlich, Appl. Opt. **33**, No. 27, 6472–6481 (1994).
16. R.G. Frehlich and M.J. Yadlowsky, J. Atmos. Ocean. Technol. **11**, 1217–1230 (1994).
17. R.G. Frehlich, S.M. Hannon, and S.W. Henderson, J. Atmos. Ocean. Technol. **11**, No. 6, 1517–1528 (1994).

18. R.G. Frehlich, J. Atmos. Ocean. Technol. **13**, 646–658 (1996).
19. R.G. Frehlich, J. Atmos. Ocean. Technol. **14**, 54–75 (1997).
20. R.G. Frehlich and L. Cornman, Appl. Opt. **38**, No. 36, 7456–7466 (1999).
21. R.G. Frehlich, J. Appl. Meteorol. **39**, 245–262 (2000).
22. R.G. Frehlich, J. Atmos. Ocean. Technol. **18**, 1749–1772 (2001).
23. R.G. Frehlich and L. Cornman, J. Atmos. Ocean. Technol. **19**, 355–366 (2002).
24. R.G. Frehlich, in: *Proc. of 12th Coherent Laser Radar Conference* (Bar Harbor Maine, US, 2003), pp. 139–142.
25. R.G. Frehlich, J. Atmos. Ocean. Technol. **21**, 905–920 (2004).
26. V.A. Banakh, F. Kopp, Ch. Werner, and I.N. Smalikho, J. Atmos. Ocean. Technol. **16**, No. 8, 1044–1061 (1999).
27. V.A. Banakh and I.N. Smalikho, Atmos. Oceanic Opt. **10**, Nos. 4–5, 295–302 (1997).
28. V.A. Banakh, Ch. Werner, F. Kopp, and I.N. Smalikho, Atmos. Oceanic Opt. **9**, No. 10, 849–853 (1996).
29. V.A. Banakh, I.N. Smalikho, F. Kopp, and Ch. Werner, Appl. Opt. **34**, No. 12, 2055–2067 (1995).
30. V.A. Banakh and I.N. Smalikho, Atmos. Oceanic Opt. **10**, No. 12, 957–965 (1997).
31. A. Leike, J. Streicher, Ch. Werner, V.A. Banakh, I.N. Smalikho, W. Wergen, and A. Cress, J. Atmos. Ocean. Technol. **18**, 1447–1456 (2001).
32. V.A. Banakh, I.N. Smalikho, and Ch. Werner, Appl. Opt. **39**, No. 33, 5393–5402 (2000).
33. V.A. Banakh, I.N. Smalikho, and Ch. Werner, Appl. Opt. **39**, No. 33, 5403–5414 (2000).
34. I.N. Smalikho, V.A. Banakh, F. Kopp, and Ch. Werner, Atmos. Oceanic Opt. **15**, No. 8, 607–614 (2002).
35. V.A. Banakh and A.V. Falits, Atmos. Oceanic Opt. **17**, No. 4, 260–267 (2004).
36. Ch. Werner, J. Streicher, O. Reitebuch, E. Nagel, T. Schneiderhan, T. König, S. Lehner, V.A. Banakh, A.V. Falits, A. Dabas, P. Delville, Atmos. Oceanic Opt. **17**, No. 8, 576–583 (2004).
37. V.A. Banakh and Ch. Werner, Opt. Eng. (2005) (to be published).
38. S. Rahm, in: *Coherent Laser Radar Conference*, Technical Digest Series **19**, 130–133 (1995).
39. A.I. Grishin and G.G. Matvienko, in: *Instruments for Remote Sensing of the Atmospheric Parameters* (Publishing House of TA SB AS SSSR, Tomsk, 1987), pp. 47–53.
40. www.idt.com
41. www.atmel.com
42. www.cirrus.com
43. R.K. Otnes and L. Enochson, *Applied Time Series Analysis*. Vol. 1. *Basic Techniques* (New York, 1978).
44. J. Postel, ed., *Internet Protocol – DARPA Internet Program Protocol Specification.* RFC 791, USC/ Information Sciences Institute (September 1981).